BRUKER

timsTOF Pro/fleX – Four reasons to switch to 4D-Proteomics™ on the timsTOF platform

If you are writing a grant and want some concise arguments for replacing older 3D mass spectrometers with the 4D capable on the timsTOF platform, download this brochure.

Click Here to Download the Brochure

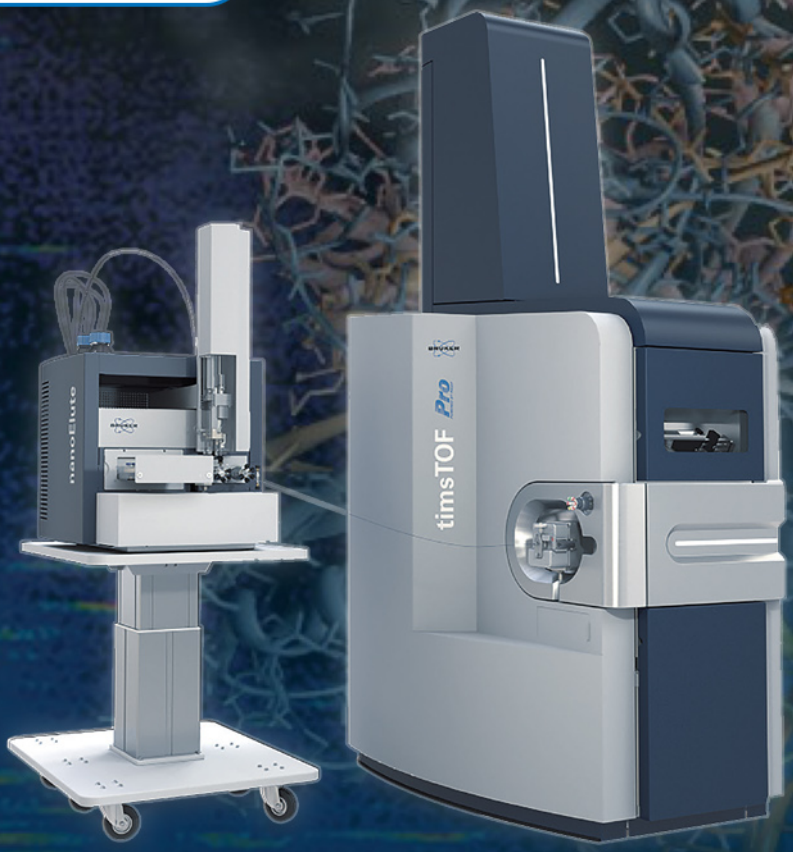

Received: 20 February 2019 | Revised: 2 July 2019 | Accepted: 2 July 2019

DOI: 10.1002/rcm.8523

SPECIAL ISSUE RESEARCH ARTICLE

WILEY Rapid Communications in Mass Spectrometry

Direct liquid extraction surface analysis mass spectrometry of cell wall lipids from mycobacteria: Salt additives for decreased spectral complexity

Alexander N. Conner | Jessie R. Jarvis | Luke J. Alderwick | Rian L. Griffiths

School of Biosciences, University of Birmingham, Edgbaston B15 2TT, UK

Correspondence
R. L. Griffiths, School of Pharmacy, University of Nottingham, Nottingham NG7 2RD, UK.
Email: rian.griffiths@nottingham.ac.uk

Funding information
Biotechnology and Biological Sciences Research Council, Grant/Award Number: BB/R017255/1; British Mass Spectrometry Society; Royal Society of Chemistry Analytical Chemistry Trust Fund, Grant/Award Number: ACSS 18/001

Rationale: Lipids are important mycobacterium cell wall constituents; changes are linked with drug resistance. Liquid extraction surface analysis (LESA) enables direct sampling in a highly sensitive manner. Here we describe protocols for the analysis of lipids from bacterial colonies. Lipids form various adducts, complicating spectra. Salt additives were investigated to circumvent this problem.

Methods: Chloroform:methanol mixtures were studied for lipid extraction and analysis by LESA-MS. The inclusion of (ESI-compatible) acetate salts of sodium, potassium or lithium in the extraction solvent was investigated.

Results: We report the detection of bacterial cell wall lipids from mycobacterial species using LESA for the first time. Sampling protocols were optimised for the use of volatile extraction solvents. The inclusion of acetate salt additives in the sampling solvent significantly reduces spectral complexity in comparison with no additives being used.

Conclusions: LESA offers a sensitive technique for bacterial lipid phenotyping. The inclusion of an acetate salt in the sampling solvent drives adduct formation towards a specific adduct type and thus significantly reduces spectral complexity.

1 | INTRODUCTION

Tuberculosis (TB) continues to be the primary cause of global morbidity and mortality caused by a single infectious agent. The etiological agent of TB, *Mycobacterium tuberculosis*, is a unique bacterial pathogen with a highly complex cell envelope that is essential for its pathogenicity, virulence and ability to combat molecular attack from host defence mechanisms and antibiotic therapy. The mycobacterial cell envelope is loaded with a complex polysaccharide, arabinogalactan, which serves to covalently connect the inner peptidoglycan layer with an outer mycolate layer that is highly hydrophobic. This complex cell wall structure has been directly linked with natural antibiotic resistance.[1] Phosphatidylinositol mannosides (PIMs) are essential phospholipid components of the cell envelope. PIMs are predominantly located in the mycobacterial plasma membrane, which is highly asymmetric and also contains other phospholipids such as phosphatidylinositol (PI), phosphatidylethanolamine (PE) and cardiolipin (CL). The PIMs appear in different glycosylation and acylation states and have been shown to play an important role in host-pathogen interactions.[2] The specific acylation states of these lipids have been linked with the initiation of granuloma formation;[3] thus, these PIM species can be considered important biomarkers with respect to healthy and *M. tuberculosis* disease state clinical samples.

Ambient ionisation is a useful tool for the direct analysis of a wide variety of biomolecules from biological samples that are not vacuum stable and thus need to be sampled under normal room conditions, such as bacterial colonies grown on agar. A wealth of

ambient ionisation techniques have been described in recent years; however, only a handful have been described for the direct analysis of bacterial colonies. Desorption electrospray ionisation (DESI), which desorbs analytes from a surface in a continuously sprayed jet of solvent ions, has recently been described for imaging of recombinant small molecule biocatalysts from *E. coli*.[4] Rapid evaporative ionisation mass spectrometry (REIMS), also known as the iKnife, which continuously ablates a sample and then detects gaseous ions removed from the sample, has been described for the analysis of phospholipids from bacterial colonies including *P. aeruginosa*, *B. subtilis*, and *S. aureus* grown on agar.[5]

Flowprobe MS, which samples a surface via a continuous solvent flow over the sample, before aspirating away and ionising via conventional electrospray ionisation (ESI), has been described for small molecule metabolites produced by a large variety of bacterial and fungal species grown on agar.[6] Finally, liquid extraction surface analysis (LESA), which probes a surface via a liquid interface formed between a conductive pipette tip and the sample surface prior to conventional ESI, has been described for the direct analysis of intact proteins from *E. coli*, *Pseudomonas aeruginosa* and *Staphylococcus aureus* grown on agar[7,8] and for lipid analysis from tissues,[9] and other surfaces.[10] This approach is of particular interest as LESA provides higher sensitivity than the three continuous ablation/extraction methods described above.

Lipids are a diverse class of molecules ranging from polar to apolar species, neutral to basic and acidic; thus different solvent systems are preferentially used to extract different classes of lipids.[11,12] Previous reports of lipid analysis of other surfaces via LESA have considered only limited extraction solvent systems, namely 4:2:1 isopropanol: methanol:chloroform with the inclusion of either ammonium acetate or formate (20 mM). LESA investigations using these solvent systems have led to the detection of wax ester species,[10] cholesterol esters and ceramides,[13] phospholipids,[13,14] and fatty acids.[14]

Lipid analysis is further complicated by the formation of multiple different adducts during the ionisation process, such as $[M+H]^+$, $[M+Na]^+$ and $[M+K]^+$. Previously, the inclusion of certain salts in the electrospray solvent has afforded simplified spectra owing to the formation of a single adduct type. The inclusion of ammonia has been shown to simplify spectra by eliminating interfering sodium adducts in previous ESI experiments.[15] Furthermore, the addition of lithium acetate to ESI solvents has been described to be optimal for lipid dissociation (MS/MS) experiments.[16] Finally, the inclusion of ammonium-based salts in DESI extraction solvents has been shown to provide benefits in purified protein analysis from glass slides.[17]

Here we describe suitable LESA extraction solvents for the direct analysis of acyl-phosphatidylinositol mannoside (Acyl-PIM) glycolipids, triacylglycerols and phosphoethanolamine species from bacterial colonies of *Mycobacterium smeglatis* (*M. smegmatis*) a bacterial model system for Mycobacterium tuberculosis. We also explore acetate salt addition to LESA extraction solvents for spectral simplification and structural characterisation, aiding accurate mass matching of lipid species directly to online mycobacterial databases. Our approach offers a rapid method for bacterial phenotyping via direct lipid analysis.

2 | EXPERIMENTAL

2.1 | Materials

All salts (lithium acetate, sodium acetate and potassium acetate) were purchased from Sigma-Aldrich (Gillingham, UK). HPLC grade chloroform and methanol were sourced from J. T. Baker (Deventer, The Netherlands). Middlebrook 7H9, Triptic Soy Broth (TSB) and Bacto Agar mycobacterial growth media were also purchased from Sigma-Aldrich.

2.2 | Bacterial sample preparation

Mycobacterium Smegmatis mc^2155 was initially inoculated into 5 mL of TSB media and cultured to an OD_{600} of 0.5. Cells were then harvested by centrifugation and resuspended in 5 mL of 7H9 media before 2-μL aliquots were inoculated onto 7H9 agar plates (6 cm, 100 mL agar), supplemented with 1.2% w/v Bacto Agar, using a dropping pipette to ensure that the colonies formed were sufficiently large enough for LESA sampling (~5 mm diameter). Agar plates were incubated at 37°C for 3–4 days and then transferred into a dark fridge environment where the temperature was kept at 5°C for storage.

2.3 | LESA sampling

LESA was carried out by use of the Triversa Nanomate (Advion Biosciences, Ithaca, NY, USA) using the advanced user interface feature. The extraction/ionisation solvent was 2:1 chloroform: methanol either with or without the inclusion of 10 mM acetate salt (lithium, sodium or potassium). During extraction, 10 μL of solvent was aspirated from the solvent well, before sampling the bacterial colony with 5 μL of this solvent for 3 s. Finally, 6 μL of the sampling solvent was re-aspirated and infused into the mass spectrometer at a gas pressure of 0.15 psi and a potential of 1.7 kV.

2.4 | Mass spectrometry

All data were acquired on an Orbitrap Elite instrument (Thermo Fisher Scientific, Waltham, MA, USA). Full scan mode data were recorded in postive ion mode at a resolution of 120,000 at *m/z* 200 between *m/z* 150 and 2000. The automatic gain control (AGC) target was 1×10^6 charges, and the maximum injection time was 1000 ms. Data were acquired for up to 2 min in full scan mode. Data were analysed by use of the Xcalibur software (version 3.0.63, Thermo Fisher Scientific). High-energy collision-induced dissociation (HCD) experiments were performed at a collision energy of 45 eV.

2.5 | Data analysis

Lipids were identified via accurate mass matching with the LIPID MAPS mycobacterial database. Experiments performed without salt addition data were searched against $[M + H]^+$, $[M + Na]^+$ and $[M + K]^+$ values. Sodium and potassium acetate experiments were searched against either $[M + Na]^+$ only or $[M + K]^+$ values only, respectively. Lithium adducts do not feature in the database; therefore, assignments made upon lithium adduct addition were searched against a calculated neutral mass after subtracting the most abundant isotopic mass of lithium from the detected *m/z* value.

3 | RESULTS

3.1 | LESA-MS sampling of lipids from bacterial colonies

Direct analysis of bacterial colonies using extraction solvents suitable for lipid analysis presents numerous challenges. Previously, intact protein species have been extracted from bacterial colonies of *E. coli*, *Pseudomonas aeruginosa* and *Staphylococcus aureus* grown on agar[7,8] using a mixture of acetonitrile and water containing formic acid. However, this was achieved via contact-LESA, by disrupting the colony. This type of analysis has also been demonstrated to allow analysis of surfaces such as tissue using volatile solvent systems that are required for lipid analysis (e.g. mixtures of chloroform, methanol and propanol).[14]

The LESA sampling regimes in these studies describe extraction times upwards of 30 s. This is not compatible with liquid-junction sampling of bacterial colonies with the volatile solvents required for lipid extraction as the solvent simply either evaporates or seeps into the colony, and the liquid-junction is lost. An extraction time of 3 s was found to be optimal when using these solvent systems and was used throughout this study. In addition, the inclusion of formic acid in the extraction solvent is not required to achieve high signal intensities (unlike typical intact protein protocols) because the lipid species detected are highly ionisable.

Sampling of the bacterial colonies with chloroform:methanol (2:1), a commonly reported lipid extraction solvent in bulk extraction experiments,[18] led to the detection of abundant lipid species in the *m/z* range 1150–1550. These species were not abundant in the background spectrum acquired from agar only (see Figure S1, supporting information). Figure 1A shows a typical mass

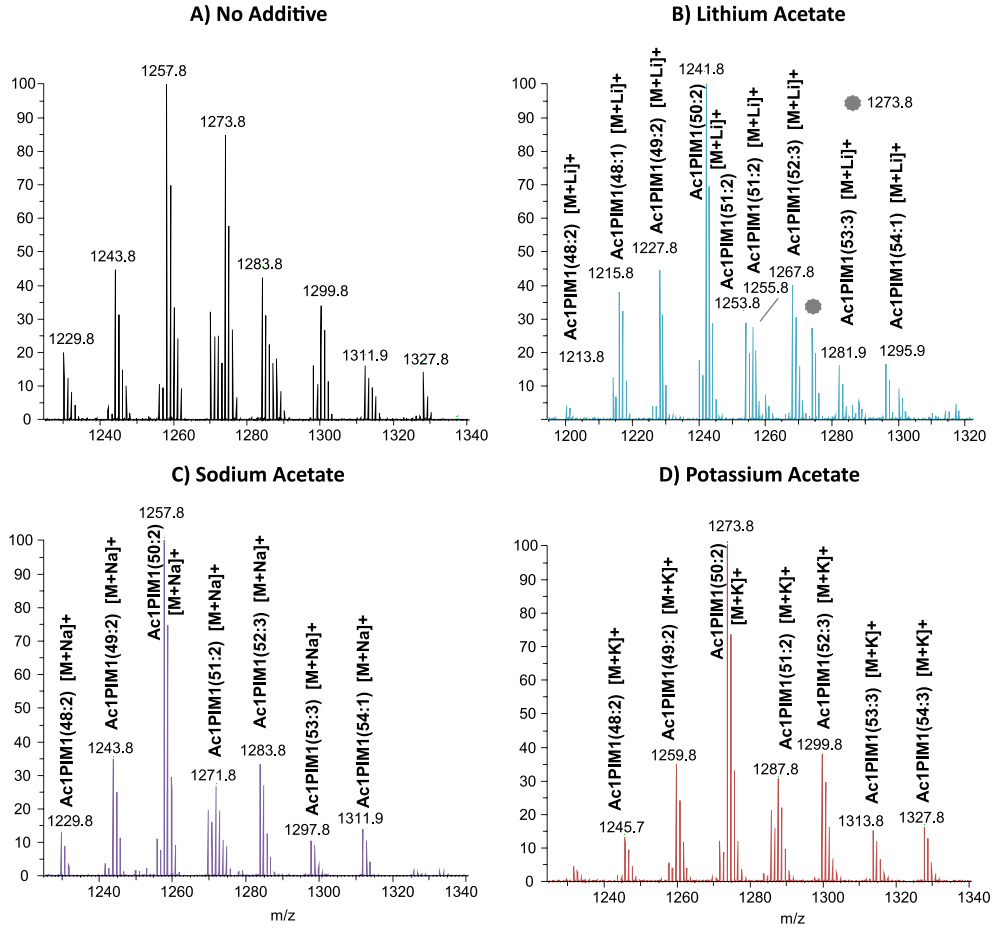

FIGURE 1 LESA-MS spectra of bacterial colonies of *M. smegmatis* sampled with chloroform:methanol sampling solvents containing A, no other additives; B, 10 mM lithium acetate; C, 10 mM sodium acetate; and D, 10 mM potassium acetate. A number of abundant Ac1PIM1 lipid species were detected in the region shown [Color figure can be viewed at wileyonlinelibrary.com]

spectrum of 1 min of summed data upon sampling of the mycobacterium with 2:1 chloroform:methanol. Lower intensity ions were detected in the phospholipid region between *m/z* 700 and 900; these are discussed in further detail below. Processing of the tabulated *m/z* values detected in the LIPID MAPS mycobacterium database[11] reveals that many of the species detected in the region *m/z* 1150–1350 are phosphatidylinositol mannoside (acyl-PIM) lipids. However, lipids form various adduct types (protonated, sodium and potassium adducts); hence, it is difficult to confidently assign which lipids are present.

The eight most abundant peaks in the *m/z* range 1220–1320 upon sampling *M. smegmatis* with chloroform:methanol (2:1) were *m/z* 1229.8, 1243.8, 1257.8, 1273.8, 1283.8, 1299.8, 1311.9 and 1327.8, as shown in Figure 1A. Searching these *m/z* values in the LIPID MAPS database against protonated, sodium and potassium adduct matches generates up to three results per *m/z* value. For example, the ion detected at *m/z* 1229.8 can be assigned as either the protonated adduct of Ac1PIM1(50:5) (−5.20 ppm deviation) or the sodium adduct of Ac1PIM1(48:2) (−7.16 ppm deviation). Similarly, the ion detected at *m/z* 1243.8 can be assigned as either the protonated adduct of Ac1PIM1(51:5) (−4.90 ppm deviation) or the sodium adduct of Ac1PIM1(49:2) (−6.83 ppm deviation) and that at *m/z* 1299.8 can be assigned as either the protonated adduct of Ac1PIM1(55:5) (−2.31 ppm deviation) or the sodium adduct of Ac1PIM1(43:2) (−4.15 ppm deviation). These examples are all within 10 ppm deviation of the accurate masses of these ions and within a few ppm of each other. It is therefore challenging, without very high mass accuracy such as that afforded by Fourier transform ion cyclotron resonance (FT-ICR) analysers, to confidently assign which lipids have been detected.

The peak at *m/z* 1257.8 can also be assigned as either the protonated adduct of Ac1PIM1(52:5) (−4.69 ppm deviation) or the sodium adduct of Ac1PIM1(50:2) (−6.60 ppm deviation); the situation is further complicated when utilising lower accurate mass instrumentation as the potassium adduct of Ac1PIM1(49:3) is predicted within just 0.06 *m/z* units or 50 ppm. It can also be possible to have a mixture of contributions; hence, it is difficult to be certain which lipids are present without reducing this spectral complexity and/or performing dissociation experiments. This complication of overlapping sodium and potassium adducts is also the case for *m/z* 1283.8 (either Ac1PIM1(52:3) or Ac1PIM1(51:4)) and *m/z* 1311.8 (either Ac1PIM1(54:3) or Ac1PIM1(53:4)).

Furthermore, peaks at *m/z* 1257.8 and 1273.8 can be tentatively assigned as the $[M + Na]^+$ and $[M + K]^+$ adducts, respectively, of the same species (AcPIM1(50:2)) based on accurate mass, see Table 1. These are two of the most abundant peaks detected and this demonstrates an inherent challenge with lipid analysis from biological samples which often contain various salts from which lipids can form cationic adducts. Any individual analyte forming multiple adducts/ions is associated with decreased sensitivity at a given *m/z* value. Thus, promoting the formation of a single adduct type to reduce spectral complexity is attractive.

In order to address these problems salt additives were introduced into the extraction solvent with the aim of directing dominant adduct formation to reduce spectral complexity and afford greater confidence in assignment by requiring searching against a single adduct type only.

3.2 | Salt additive addition to extraction solvents for spectral simplification

The addition of 10 mM lithium, sodium or potassium acetate to the sampling solvent led to a shift in dominant adduct formation to the respective cationic adduct and thus much reduced spectral complexity. Note that only acetate salts were investigated in this study as they are volatile salts that are compatible with the ESI process; other salt forms are less appropriate for electrospray based techniques as they reduce sensitivity.[19] For brevity, trends observed upon salt addition will be described for the most abundant ions only; a full list of detected lipids is provided in Table 1.

The inclusion of lithium acetate in the LESA sampling solvent led to a change in the abundant *m/z* values detected from the bacterial colony. Figure 1B shows representative mass spectra from the lithium acetate additive experiment. Peaks corresponding to the lithium adducts of the seven most abundant Ac1PIM1 species: (48:2), (49:2), (50:2), (51:2), (52:3), (53:3) and (54:1) were detected at *m/z* 1213.8, 1227.8, 1241.8, 1255.8, 1267.8, 1281.9 and 1295.9, respectively. The inclusion of sodium acetate in the extraction solvent led to the detection of dominant peaks at *m/z* 1229.8, 1243.8, 1257.8, 1271.8, 1283.8, 1297.8 and 1311.9 corresponding to sodium adducts of the same Ac1PIM1 species: (48:2), (49:2), (50:2), (51:2), (52:3), (53:3) and (54:1), respectively, see Figure 1C. It should be noted that searching these masses in the LIPID MAPS mycobacterial database returns just one result (as sodium adducts). When potassium acetate was included in the sampling solvent dominant peaks were detected at *m/z* 1245.7, 1259.8, 1273.8, 1287.8, 1299.8, 1313.8 and 1327.8, corresponding to a mass shift of 16 Da in comparison with the sodium acetate experiment and potassium adducts of the same seven Ac1PIM1 species as described above, see Figure 1D.

Driving adduct formation to a specific cationic adduct helps confirm that the dominant peaks in the control experiment are a mixture of adduct types; *m/z* 1257.8 was the most abundant peak in the spectrum. However, it is not detected in high abundance when potassium acetate is included in the sampling solvent; thus, it can be confirmed as the sodium adduct Ac1PIM1(50:2) rather than the potassium adduct of Ac1PIM1(49:1). This becomes particularly important for assignments made on lower accurate mass instrumentation where up to three adducts are detected within a small *m/z* window. Conversely, the peak at *m/z* 1273.8 (the second most abundant peak in this *m/z* region) is not present in high abundance in the sodium acetate experiment and can be confirmed as the potassium adduct of the same lipid (Ac1PIM1(50:2)). The fact that the same abundant species were detected in each experiment provides good confidence of these assignments; thus, inclusion of a salt in the sampling solvent simplifies analysis.

TABLE 1 Lipid species assigned by LIPID MAPS mycobacterial database mass matching (within 10 ppm deviation of the accurate mass) in the region *m/z* 1200–1350 upon sampling *M. smegmatis* with 2:1 chloroform:methanol. Matched peak masses that correspond to more than one match are highlighted in bold

Detected mass	Matched mass	Assignment	Adduct	Deviation (ppm)	Detected mass	Matched mass	Assignment	Adduct	Deviation (ppm)
1215.7611	1215.7505	Ac1PIM1(47:2)	$[M + Na]^+$	−8.72	**1279.8704**	1279.8699	CL(59:2)	$[M + H]^+$	−0.39
1229.7750	1229.7662	Ac1PIM1(48:2)	$[M + Na]^+$	−7.16	**1279.8704**	1279.8781	Ac1PIM1(53:1)	$[M + H]^+$	6.02
1229.7750	1229.7686	Ac1PIM1(50:5)	$[M + H]^+$	−5.20	1283.7680	1283.7558	Ac1PIM1(51:4)	$[M + K]^+$	−9.50
1231.7709	1231.7818	Ac1PIM1(48:1)	$[M + Na]^+$	8.85	1283.8211	1283.8131	Ac1PIM1(52:3)	$[M + Na]^+$	−6.23
1231.7331	1231.7245	Ac1PIM1(47:2)	$[M + K]^+$	−6.98	1285.7792	1285.7714	Ac1PIM1(51:3)	$[M + K]^+$	−6.07
1233.7382	1233.7401	Ac1PIM1(47:1)	$[M + K]^+$	1.54	**1285.8279**	1285.8312	Ac1PIM1(54:5)	$[M + H]^+$	2.57
1235.8248	1235.8155	Ac1PIM1(50:2)	$[M + H]^+$	−7.53	**1285.8279**	1285.8288	Ac1PIM1(52:2)	$[M + Na]^+$	0.70
1239.8395	1239.8468	Ac1PIM1(C50)	$[M + H]^+$	5.89	1287.7943	1287.7871	Ac1PIM1(51:2)	$[M + K]^+$	−5.59
1241.7753	1241.7662	Ac1PIM1(49:3)	$[M + Na]^+$	−7.33	1289.8012	1289.8027	Ac1PIM1(51:1)	$[M + K]^+$	1.16
1243.7330	1243.7245	Ac1PIM1(48:3)	$[M + K]^+$	−6.83	1297.7793	1297.7714	Ac1PIM1(52:4)	$[M + K]^+$	−6.09
1243.7903	1243.7842	Ac1PIM1(51:5)	$[M + H]^+$	−4.90	1297.8371	1297.8288	Ac1PIM1(53:3)	$[M + Na]^+$	−6.40
1243.7903	1243.7818	Ac1PIM1(49:2)	$[M + Na]^+$	−6.83	1299.7948	1299.7871	Ac1PIM1(52:3)	$[M + K]^+$	−5.92
1245.7483	1245.7401	Ac1PIM1(48:2)	$[M + K]^+$	−6.58	**1299.8498**	1299.8444	Ac1PIM1(53:2)	$[M + Na]^+$	−4.15
1245.7953	1245.7999	Ac1PIM1(51:4)	$[M + H]^+$	3.69	**1299.8498**	1299.8468	Ac1PIM1(55:5)	$[M + H]^+$	−2.31
1245.7953	1245.7975	Ac1PIM1(49:1)	$[M + Na]^+$	1.77	1301.8023	1301.8027	Ac1PIM1(52:2)	$[M + K]^+$	0.31
1247.7533	1247.7558	Ac1PIM1(48:1)	$[M + K]^+$	2.00	**1303.8146**	1303.8101	CL(58:2)	$[M + K]^+$	−3.45
1253.8534	1253.8625	Ac1PIM1(C51)	$[M + H]^+$	7.26	**1303.8146**	1303.8184	Ac1PIM1(52:1)	$[M + K]^+$	2.91
1255.7898	1255.7818	Ac1PIM1(50:3)	$[M + Na]^+$	−6.37	1311.7960	1311.7871	Ac1PIM1(53:4)	$[M + K]^+$	−6.78
1257.7495	1257.7401	Ac1PIM1(49:3)	$[M + K]^+$	−7.47	1311.8524	1311.8444	Ac1PIM1(54:3)	$[M + Na]^+$	−6.10
1257.8058	1257.7999	Ac1PIM1(52:5)	$[M + H]^+$	−4.69	1313.8106	1313.8027	Ac1PIM1(53:3)	$[M + K]^+$	−6.01
1257.8058	1257.7975	Ac1PIM1(50:2)	$[M + Na]^+$	−6.60	**1315.8188**	1315.8101	CL(59:3)	$[M + K]^+$	−6.61
1259.7638	1259.7558	Ac1PIM1(49:2)	$[M + K]^+$	−6.35	**1315.8188**	1315.8184	Ac1PIM1(53:2)	$[M + K]^+$	−0.30
1259.8093	1259.8155	Ac1PIM1(52:4)	$[M + H]^+$	4.92	1317.8342	1317.8258	CL(59:2)	$[M + K]^+$	−6.37
1259.8093	1259.8131	Ac1PIM1(50:1)	$[M + Na]^+$	3.02	1317.8342	1317.8340	Ac1PIM1(53:1)	$[M + K]^+$	−0.15
1261.7694	1261.7714	Ac1PIM1(49:1)	$[M + K]^+$	1.59	1325.8093	1325.8027	Ac1PIM1(54:4)	$[M + K]^+$	−4.98
1267.8695	1267.8781	Ac1PIM1(C52)	$[M + H]^+$	6.78	1325.8665	1325.8601	Ac1PIM1(55:3)	$[M + Na]^+$	−4.83
1269.7504	1269.7401	Ac1PIM1(50:4)	$[M + K]^+$	−8.11	1325.9566	1325.9481	Cl(C62)	$[M + H]^+$	−6.41
1269.8064	1269.7975	Ac1PIM1(51:3)	$[M + Na]^+$	−7.01	1327.8261	1327.8184	Ac1PIM1(54:3)	$[M + K]^+$	−5.80
1271.7640	1271.7558	Ac1PIM1(50:3)	$[M + K]^+$	−6.45	**1329.8317**	1329.8258	CL(60:3)	$[M + K]^+$	−4.44
1271.8190	1271.8155	Ac1PIM1(53:5)	$[M + H]^+$	−2.75	**1329.8317**	1329.8340	Ac1PIM1(54:2)	$[M + K]^+$	1.73
1271.8190	1271.8131	Ac1PIM1(51:2)	$[M + Na]^+$	−4.64	1331.8359	1331.8414	CL(60:2)	$[M + K]^+$	4.13
1273.7791	1273.7714	Ac1PIM1(50:2)	$[M + K]^+$	−6.05	1341.8421	1341.8340	Ac1PIM1(55:3)	$[M + K]^+$	−6.04
1275.7846	1275.7871	Ac1PIM1(50:1)	$[M + K]^+$	1.96	**1343.8473**	1343.8414	CL(61:3)	$[M + K]^+$	−4.39
					1343.8473	1343.8497	Ac1PIM1(55:2)	$[M + K]^+$	1.79

However, when lithium acetate was included in the sampling solvent a number of peaks were dominant in the region *m/z* 1200–1320 that were not assigned via the searches. For example, *m/z* 1273.8 corresponds to the potassium adduct of the most abundant species in this region (Ac1PIM1(50:2) $[M + K]^+$). Thus, the inclusion of lithium acetate in the LESA sampling solvent did not provide the same degree of spectral simplification as that described above when either sodium or potassium acetate was incorporated.

The inclusion of salt additives in MALDI matrices has become a commonplace approach for spectral simplification through directing lipid adduct formation.[20] Previous ESI studies have utilised acetate salts to drive adduct formation towards a desired lipid adduct for phosphocholine and triacylglycerol species;[16] however, this methodology has not previously been described for the LESA of lipids directly extracted from biological samples. The inclusion of ammonium salt additives in sampling solvents for DESI-MS analysis of intact proteins has been shown to increase sensitivity.[17] The salt additive approach in this study has enabled assignment (by reducing matches to a single result from a single adduct type and based on accurate mass only) of the detection of 20 different acyl-phosphatidylinositol mannoside species in agreement across three experiments, as shown in Table 2. There is also evidence of cardiolipin species which are important structural cell membrane components that enable cell curvature and represent an attractive drug target.[21] Here we show for the first time that similar approaches can be extended to LESA and for the analysis of biologically relevant bacterial cell wall lipids. It should be noted that certain cardiolipin species and acyl-phosphatidylinositol mannoside species have masses within a few ppm of one another and therefore cannot be distinguished from one another without structural characterisation.

Although these experiments targeted analysis of acyl-phosphatidylinositol mannoside lipids (and these were the most abundant species detected in this study) a number of other lipid species were also indicated from the LIPID MAPS database searches. In the region *m/z* 700–900 a total of nine phosphatidylethanolamine assignments within 5 ppm accurate mass were suggested by the

TABLE 2 Lipid species detected across salt additive experiments (lithium, sodium and potassium acetate addition). Deviation (ppm) is shown as an average of three values

Neutral mass (Da)	Assignment	Deviation (ppm)	Neutral mass (Da)	Assignment	Deviation (ppm)
689.4996	PE(32:1)	4.83	1192.7613	Ac1PIM1(47:2)	−7.16
691.5152	PE(32:0)	0.83	1194.8402	Ac1PIM1(47:1)	2.94
705.5308	PE(33:0)	0.60	1206.7770	Ac1PIM1(48:2)	−6.90
715.5152	PE(34:2)	1.78	1208.7926	Ac1PIM1(48:1)	−1.14
717.5308	PE(34:1)	1.36	1218.777	Ac1PIM1(49:3)	−7.40
719.5465	PE(34:0)	1.00	1220.7926	Ac1PIM1(49:2)	−6.66
733.5621	PE(35:0)	1.11	1222.8083	Ac1PIM1(49:1)	1.26
745.5621	PE(36:1)	0.36	1232.7926	Ac1PIM1(50:3)	−6.60
774.6737	TG(46:2)	1.48	1234.8083	Ac1PIM1(50:2)	−6.40
775.6091	PE(C38)	1.40	1236.8239	Ac1PIM1(50:1)	1.19
776.6894	TG(46:1)	1.18	1246.8083	Ac1PIM1(51:3)	−6.26
778.7050	TG(C46)	2.35	1248.8239	Ac1PIM1(51:2)	−5.85
786.6314	MK-9(C)	2.34	1250.8396	Ac1PIM1(51:1)	0.73
790.7050	TG(47:1)	1.42	1258.8083	Ac1PIM1(52:4)	−7.70
792.7207	TG(47:0)	1.44	1260.8239	Ac1PIM1(52:3)	−6.22
800.6894	TG(48:3)	1.53	1262.8396	Ac1PIM1(52:2)	−1.02
802.7050	TG(48:2)	2.11	1264.8552/1264.8470	Ac1PIM1(52:1)/CL(58:2)	−1.85/−4.56
804.7207	TG(48:1)	0.85	1274.8396	Ac1PIM1(53:3)	−6.38
806.7363	TG(48:0)	1.51	1276.8552	Ac1PIM1(53:2)/CL(59:3)	−1.68/−6.61
818.7363	TG(49:1)	1.44	1278.8708	Ac1PIM1(53:1)/CL(59:2)	2.30/4.84
820.7520	TG(49:0)	2.15	1288.8552	Ac1PIM1(54:3)	−6.16
828.7207	TG(50:3)	0.98	1290.8709/1290.8626	Ac1PIM1(54:2)/CL(60:3)	0.68/−5.96
830.7363	TG(50:2)	1.02	1292.9498	Ac2SGL(C71)	3.15
832.7520	TG(50:1)	0.90	1302.8709	Ac1PIM1(55:3)	−6.43
844.7520	TG(51:2)	2.16	1304.8782	CL(61:3)	−5.66
846.7676	TG(51:1)	1.04	1304.8865	Ac1PIM1(55:2)	0.52
848.7832	TG(51:0)	1.27			
856.7520	TG(52:3)	1.14			
858.7676	TG(52:2)	0.99			
860.7832	TG(52:1)	0.68			

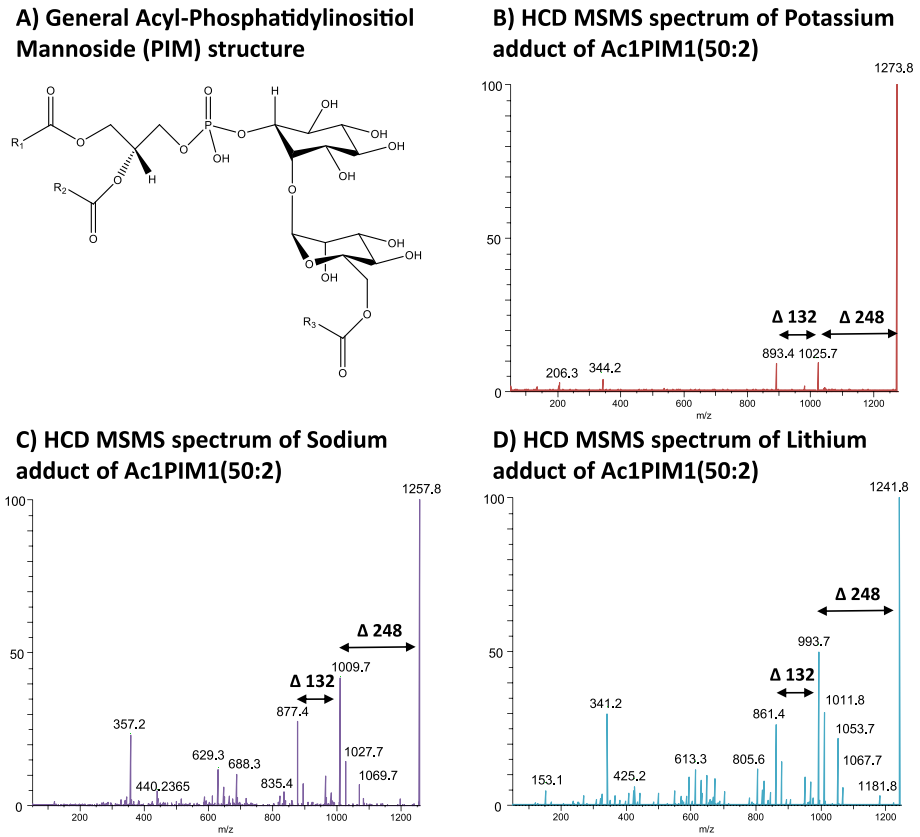

FIGURE 2 A, Generic structure of an acyl phosphatidylinositol mannoside (Ac1PIM1) lipid. Example LESA-HCDMSMS mass spectra of B, the potassium adduct ion; C, the sodium adduct ion; and D, the lithium adduct ion of Ac1PIM1(50:2) detected from *M. smegmatis* [Color figure can be viewed at wileyonlinelibrary.com]

LIPID MAPS mycobacterial database in at least two of three repeats, as shown in Table 2. Furthermore, twenty triacylglycerol species were also suggested. These lipid classes also comprise part of the complex cell wall structure of mycobacterium and present biomolecularly informative ions for bacterial phenotyping and/or monitoring bacterial stress.

3.3 | Improved structural information

The addition of salt additives to promote a specific adduct type was also used to investigate the extent of structural information afforded from each adduct type via high-energy collision-induced dissociation (HCD). Figure 2 shows the generic structure of an acyl-phosphatidylinositol mannoside species and the HCD spectra obtained after fragmentation of the $[M+K]^+$, $[M+Na]^+$ and $[M+Li]^+$ adducts of Ac1PIM1(50:2). Only four major product ions were detected upon dissociation of the potassium adduct, indicating that this adduct is relatively stable. A greater degree of dissociation is observed upon dissociation of the $[M+Na]^+$ adduct and further still upon dissociation of the $[M+Li]^+$ adduct. It is of note that there are a greater number of product ions between *m/z* 400 and 850 in the lithium and sodium experiments which are probably indicative of fatty acid side-chain losses, which have been reported from other phospholipid backbones. This trend, that smaller cationic adducts give rise to richer lipid fragmentation data, has been described previously;[22] here we describe the same benefits for acyl-phosphatidylinositol mannoside species.

Dissociation of each adduct type gave rise to the neutral loss of 248 Da followed by the neutral loss of a further 132 Da. This is a clear trend indicative of a common fragmentation pattern; however, these are not easily deduced from the generic structure. These neutral losses were observed upon dissociation of the same adducts of at least three different species assigned as acyl-phosphatidylinositol mannosides by the LIPID MAPS database. This type of lipid species is not readily commercially available; therefore, it was not possible to compare this data with that from a purified standard. Similar ESI-HCD analysis of lithium adducts of a phosphatidylinositol lipid standard (data not shown) gave rise to neutral losses indicative of the fatty acid side-chain losses and a neutral loss of 162 Da arising from the neutral loss of inositol after the loss of water. These did not, however, aid assignment of the neutral losses or product ions detected upon dissociation of the acyl-phosphatidylinositol mannoside species. Further investigations are required to better understand the mechanisms of dissociation of these particular lipid species.

4 | CONCLUSIONS

Here we show suitable volatile extraction solvents and rapid sampling regimes for the extraction and analysis of lipid species directly from

mycobacterium. In this way, acyl-phosphatidylinositol mannoside (Acyl-PIM) lipids, which are important cell wall constituents that have been implicated in drug-resistance, can be detected. Lipids form multiple different adduct types, complicating assignments. We present salt inclusion in LESA sampling solvents as an approach to promoting formation of a particular adduct type, thus decreasing spectral complexity. This simultaneously improves mass matching with available databases as much greater confidence in the lipid adduct type significantly reduces overlapping *m/z* values of different lipids in different adduct forms. Using this approach, we report the following assignments from the LIPID MAPS mycobacterial database: twenty acyl-phosphatidylinositol mannosides, nine phosphatidylethanolamines, twenty triacylglycerols, and at least one cardiolipin. These results show great promise for the sensitive analysis of bacterial lipids that can be assigned confidently based on accurate mass supported by driving adduct formation to a specific adduct type. High-energy collision-induced dissociation studies show that lithium adducts provide rich, albeit complex, dissociation data. Future work will focus on monitoring bacterial stress via changes in lipid signals upon drug treatments and understanding the data obtained upon HCD fragmentation for the structural characterisation of these complex lipids.

ACKNOWLEDGEMENTS

RLG was funded by EPSRC (EP/L023490/1). LJA would like to acknowledge support from BBSRC (BB/R017255/1). This work was also supported via summer studentships awarded by the Royal Society of Chemistry's Analytical Chemistry Trust Fund (ACSS 18/001) and the British Mass Spectrometry Society. The authors would also like to thank Professor Helen J. Cooper for access to instrumentation.

ORCID

Luke J. Alderwick https://orcid.org/0000-0002-1257-6053
Rian L. Griffiths https://orcid.org/0000-0002-1601-4664

REFERENCES

1. Jarlier V, Nikaido H. Mycobacterial cell wall: Structure and role in natural resistance to antibiotics. *FEMS Microbiol Lett*. 1994;123(1–2):11-18.
2. Guerin ME, Kaur D, Somashekar BS, et al. New insights into the early steps of phosphatidylinositol mannoside biosynthesis in mycobacteria: PimB′ is an essential enzyme of *Mycobacterium smegmatis*. *J Biol Chem*. 2009;284(38):25687-25696.
3. Gilleron M, Ronet C, Mempel M, Monsarrat B, Gachelin G, Puzo G. Acylation state of the phosphatidylinositol mannosides from Mycobacterium bovis bacillus Calmette Guérin and ability to induce granuloma and recruit natural killer T cells. *J Biol Chem*. 2001;276(37):34896-34904.
4. Yan C, Parmeggiani F, Jones EA, et al. Real-time screening of biocatalysts in live bacterial colonies. *J Am Chem Soc*. 2017;139(4):1408-1411.
5. Golf O, Strittmatter N, Karancsi T, et al. Rapid evaporative ionization mass spectrometry imaging platform for direct mapping from bulk tissue and bacterial growth media. *Anal Chem*. 2015;87(5):2527-2534.
6. Hsu C-C, ElNaggar MS, Peng Y, et al. Real-time metabolomics on living microorganisms using ambient electrospray ionization flow-probe. *Anal Chem*. 2013;85(15):7014-7018.
7. Randall EC, Bunch J, Cooper HJ. Direct analysis of intact proteins from *Escherichia coli* colonies by liquid extraction surface analysis mass spectrometry. *Anal Chem*. 2014;86(21):10504-10510.
8. Kocurek KI, Stones L, Bunch J, May RC, Cooper HJ. Top-down LESA mass spectrometry protein analysis of gram-positive and gram-negative bacteria. *J Am Soc Mass Spectrom*. 2017;28(10):2066-2077.
9. Griffiths RL, Sarsby J, Guggenheim EJ, et al. Formal lithium fixation improves direct analysis of lipids in tissue by mass spectrometry. *Anal Chem*. 2013;85(15):7146-7153.
10. Brown SH, Huxtable LH, Willcox MD, Blanksby SJ, Mitchell TW. Automated surface sampling of lipids from worn contact lenses coupled with tandem mass spectrometry. *Analyst*. 2013;138(5):1316-1320.
11. Fahy E, Sud M, Cotter D, Subramaniam S. LIPID MAPS online tools for lipid research. *Nucleic Acids Res*. 2007;35Web Server issue:W606-W612.
12. Fahy E, Subramaniam S, Murphy RC, et al. Update of the LIPID MAPS comprehensive classification system for lipids. *J Lipid Res*. 2009;50(Suppl):S9-S14.
13. Ellis SR, Ferris CJ, Gilmore KJ, Mitchell TW, Blanksby SJ, in het Panhuis M. Direct lipid profiling of single cells from inkjet printed microarrays. *Anal Chem*. 2012;84(22):9679-9683.
14. Almeida R, Berzina Z, Arnspang EC, et al. Quantitative spatial analysis of the mouse brain lipidome by pressurized liquid extraction surface analysis (PLESA). *Anal Chem*. 2015;87:1749-1756.
15. Koivusalo M, Haimi P, Heikinheimo L, Kostiainen R, Somerharju P. Quantitative determination of phospholipid compositions by ESI-MS: Effects of acyl chain length, unsaturation, and lipid concentration on instrument response. *J Lipid Res*. 2001;42(4):663-672.
16. Hsu F-F, Turk J. Structural characterization of triacylglycerols as lithiated adducts by electrospray ionization mass spectrometry using low-energy collisionally activated dissociation on a triple stage quadrupole instrument. *J Am Soc Mass Spectrom*. 1999;10(7):587-599.
17. Honarvar E, Venter AR. Ammonium bicarbonate addition improves the detection of proteins by desorption electrospray ionization mass spectrometry. *J Am Soc Mass Spectrom*. 2017;28(6):1109-1117.
18. Folch J, Lees M, Sloane Stanley GH. A simple method for the isolation and purification of total lipids from animal tissues. *J Biol Chem*. 1957;226(1):497-509.
19. Iavarone AT, Udekwu OA, Williams ER. Buffer loading for counteracting metal salt-induced signal suppression in electrospray ionization. *Anal Chem*. 2004;76(14):3944-3950.
20. Griffiths RL, Bunch J. A survey of useful salt additives in matrix-assisted laser desorption/ionization mass spectrometry and tandem mass spectrometry of lipids: Introducing nitrates for improved analysis. *Rapid Commun Mass Spectrom*. 2012;26(13):1557-1566.
21. Jackson M, Crick DC, Brennan PJ. Phosphatidylinositol is an essential phospholipid of mycobacteria. *J Biol Chem*. 2000;275(39):30092-30099.
22. Stübiger G, Belgacem O. Analysis of lipids using 2,4,6-trihydroxyacetophenone as a matrix for MALDI mass spectrometry. *Anal Chem*. 2007;79(8):3206-3213.

SUPPORTING INFORMATION

Additional supporting information may be found online in the Supporting Information section at the end of the article.

How to cite this article: Conner AN, Jarvis JR, Alderwick LJ, Griffiths RL. Direct liquid extraction surface analysis mass spectrometry of cell wall lipids from mycobacteria: Salt additives for decreased spectral complexity. *Rapid Commun Mass Spectrom*. 2019;1–9. https://doi.org/10.1002/rcm.8523